NASA
Technical
Paper
2407

1985

Circuit Transients Due to Negative Bias Arcs on a High-Voltage Solar Array in Low Earth Orbit

Roger N. Metz

Lewis Research Center
Cleveland, Ohio

National Aeronautics
and Space Administration

Scientific and Technical
Information Branch

Summary

Arcing to negatively biased, exposed solar cell interconnects on solar arrays placed in plasma environments has been well established in laboratory tests and inferred from space data. Such arcing may cause damaging interference with the operation of electrical power systems in spacecraft planned to be driven with high-voltage solar arrays. A simple analytical model has been developed to estimate the effects of negative bias arcs on solar array power system performance. Solar cell characteristics, plasma interactions, and power system features are modeled approximately by a linear, lumped element transient circuit, and the time domain equations are solved. Exact numerical results for solar array common-mode and load voltage transients are calculated for typical conditions. Acceptable load transients are found for a range of arc current amplitudes and time constants.

Introduction

Laboratory and flight tests of small, externally biased solar cell arrays show that arcs occur on or near negatively biased solar cell interconnects exposed to plasmas typical of low Earth orbit (LEO) (refs. 1 to 4). The voltage threshold of these arcs appears to lie several hundred volts below the plasma ground potential. The large solar arrays desired for future space missions in LEO will have areas operating at voltages more negative than this threshold, if their terminal voltages are sufficiently high (ref. 5). This is especially true if the arrays are permitted to float electrically in the space plasma. Negative bias arcing is a threat to the operation of such arrays if it can be shown that unacceptable electrical transients in the power system due to arcing cannot be avoided. Conversely, arcing may be tolerated if transients and other arc effects are found to be or can be made minimal.

In order to estimate the severity of transients produced by negative bias arcs, a circuit model of a simple solar array power system has been developed. It shows approximately how load transients due to arcs on an array in LEO depend on plasma parameters, stored charge, solar cell behavior, and arc characteristics. Suitable linearizations permit a completely analytical solution to be obtained in the time domain.

The model is current driven. Current pulses are injected at the negative end of an illuminated and loaded solar array that is in prior electrical equilibrium with the plasma. A pulse causes a positive, common-mode voltage transient of the array circuit relative to the plasma and perturbs the solar cell currents and voltages so as to produce a transient across the load. The size of this transient depends in part on the operating points of the solar cells. In this report we assume operation on the high-voltage side of the maximum power point where the internal dynamic resistance of the cells is low. Operation at other points can be accommodated by the model but is expected to result in much larger voltage transients (see the **Solar Cell and Solar Array Characteristics** and the **Results and Discussion** sections.)

Several features of the model establish it as a worst-case analysis. First, the arc injection point is placed at the negative end of the array where it is expected, theoretically, to cause larger transients than if placed at more positive points. Second, the spatial distribution of the plasma interaction with the array is approximated by lumped circuit elements arranged to allow upper-bound estimates of load transients. Third, the load is assumed to be purely resistive. The filtering expected to be included in actual power system loads is withheld. These features permit a rather simple model to be made, one that is useful for probing the space of arc current parameters yielding acceptable load transients on a given array under various conditions.

Solar Cell and Solar Array Characteristics

A solar array consisting of M parallel chains of matched solar cells is assumed. Each chain contains N cells wired in series, and each chain is connected at its ends to other chains. Arcs injected at one end of the chains cause equal voltage distributions along them. Therefore, cross wiring between adjacent points of the chains is omitted. Furthermore, model linearity requires that the solar cells not be permitted to depart greatly from their quiescent operating points during a transient. Limiting the arc current amplitude achieves this and

makes modeling of reverse biasing, short- and open-circuiting of solar cells, and diode protection unnecessary.

If the array is illuminated and loaded so that each cell operates at quiescent voltage and current (ϵ_o and i_o), then the terminal voltage V_T^o is $N\epsilon_o$, the output current I_o is Mi_o, the output power is $MN\epsilon_o i_o$, and the load resistance R_L is $N\epsilon_o/Mi_o$. For small fluctuations about the operating point, the terminal voltage is given by

$$V_T = V_T^o - \rho_o(I - I_o) \tag{1}$$

where $\rho_o = N\rho/M$ and ρ is the magnitude of the dynamic resistance $d\epsilon/di$ at the operating point of a single cell having current/voltage characteristic $\epsilon(i)$. In the model, transient currents are confined to those for which equation (1) is a good approximation.

The characteristic for a silicon solar cell may be approximated by the function

$$\epsilon(i) = a(\ln\,(b - i)) + c$$

where, for a 2 cm by 2 cm cell at normal operating temperature under full solar illumination, the values $a = 40$ mV, $b = 132$ mA, and $c = 355$ mV apply (ref. 6). At full power, an array of such cells having $N = 1000$ and $M = 1500$ produces 82 kW at 450 V with $R_L = \rho_o = 2.5$ ohms. At the high-voltage 80-percent power point, which is a typical operating point used for model calculations, the array produces 66 kW of power at 508 V with $R_L = 4$ ohms and $\rho_o = 0.6$ ohm. Operation on the high current side of maximum power should be avoided in real power systems if large arcs are expected. (See the **Results and Discussion** section.)

A silicon solar cell has an internal capacitance that appears in parallel with ρ. For 2 cm by 2 cm silicon cells, $C \approx 0.02$ μF. Thus, the impedance due to C becomes important, as compared with ρ, only for pulses lasting about a microsecond or less. Although such short pulses are seen infrequently in laboratory tests, pulses with very short rise times do occur. Therefore, C must be included to model their responses correctly.

Plasma Interactions

Plasma Current Collection

The plasma environment used in this report is that of the ionosphere a near 400-km altitude (ref. 7). Plasma densities in this region rise to 10^5 or 10^6 cm^{-3}, and electron and ion mean thermal energies are a few tenths of an electron volt. The ions are O^+, predominantly. Both the Debye length and the electron gyroradius are greater than a centimeter. The electron plasma frequency exceeds 1 MHz.

A solar array placed in such an environment draws current from the plasma to the exposed metallic interconnects. Inasmuch as the interconnects are small compared to the Debye length and electron gyroradius, one might expect orbit-limited Langmuir probe theory to give an adequate estimation of current collection from the plasma. For electrons this theory predicts currents to a sphere at voltage V to be proportional to the collecting area, the electron thermal current density, and the factor $(1 + eV/kT_e)$. Ion collection in this theory is somewhat more involved (ref. 8).

Experimentally the situation is not so simple. Whereas currents to negatively biased interconnects appear to vary roughly linearly with voltage, those to positively biased interconnects are highly nonlinear. They vary as $(V - V_o)^p$ where $p \approx 1/2$ at low voltage, $p > 1$ in a *snap-over* region (ref. 1) where secondary emission effects on the cover slides become important, and $p \approx 1$ at high voltage. However, since snap-over is known experimentally to require seconds to develop, it is unlikely to play a role in the plasma response to the micro- and millisecond arcs expected. Thus, the voltage dependence of electron collection may be much more slowly varying on these time scales than is indicated by the quasistatic measurements in which snap-over is seen. The exact dependence is not yet well understood experimentally.

To make progress toward an analytical model, simplifying assumptions regarding plasma current collection must be made. The most helpful is that both electron and ion plasma currents are ohmic, i.e., proportional to voltage. Such currents are characterized by conductances α that depend on the properties of the ambient plasma and on the collecting area per cell. This is the equivalent of orbit-limited, spherical Langmuir probe collection in a thermal plasma with $eV >> kT$. Since $eV >> kT$ almost everywhere on a high voltage array in LEO, the ohmic assumption treats ion collection realistically but ignores electron snap-over.

We will assume for species s (electrons or O^+ ions) that

$$I_s = \alpha_s V \tag{2}$$

where

$$\alpha_s = e^2 j_s \frac{A}{kT_s}$$

and

$$j_s = 0.5 n_s \left(\frac{2kT_s}{\pi m_s}\right)^{1/2}$$

The plasma is assumed to be Maxwellian; n_s is the particle density; T_s and m_s are the temperature and particle mass; A is the collecting area per cell; and j_s is the ambient thermal current density. Typical values of the parameters used in the model are $n_e = n_i = 4 \times 10^5$ cm^{-3}, $kT_e = 0.2$ eV $= 2kT_i$, and $A = 1$ cm^2. Then, $\alpha_e = 2.4 \times 10^{-6}$ mho for the electrons, and $\alpha_i = 2 \times 10^{-8}$ mho for the ions.

In solar array orientations where ram ion currents to negative interconnects dominate the thermal ion currents, the previous formulation requires adjustment. It may be assumed that ion collection is then given by spherical Langmuir probe theory in a streaming plasma in the limit where $eV >> E_o$ (ion ram energy). Thus,

$$I_r = \alpha_r V \tag{3}$$

where

$$\alpha_r = e^2 A n_i \left(\frac{2}{m_i E_o} \right)^{1/2}$$

The ram ion energy for O^+ at 400 km is about 5 eV. This value gives $\alpha_r = 10^{-8}$ mho. Thus, for this case, ram ion collection is not radically different in magnitude than thermal ion collection, and numerical results for this case will not be given.

Stored Charge

The several parts of a solar cell in an array are capacitively coupled to each other and to the surrounding plasma. Substrate to cover slide, cover slide to plasma sheath, and interconnect to sheath capacitances in series/parallel combination form an equivalent capacitance per cell (C_p). An estimate of this capacitance lies in the range 1 to 200 pF for standard 2 cm by 2 cm silicon cells. The low value is approximately the capacitance to space of a sphere having area equal to that of one interconnect. The high value is the capacitance of a 2 cm by 2 cm cover slide to its substrate. Which of these limits dominates C_p depends on whether a cover slide can maintain itself near the plasma potential during an arc by charging from the plasma. If so, C_p tends toward the higher limit. Because experimental values are not yet well known, the present calculations draw upon the whole range of C_p.

Floating Equilibrium

On a self-biased solar array in electrical equilibrium with the space plasma, the electron versus ion current balance condition determines what fraction of the array lies above the plasma potential and what fraction below. Those areas above the plasma potential collect electrons and those below collect ions, almost exclusively. In the ohmic collection approximation, the conductances α_e and α_i determine how the array floats electrically. For $\alpha_e = 2.4 \times 10^{-6}$ mho and $\alpha_i = 2 \times 10^{-8}$ mho an array will float with about 8 percent of its area positive (see appendix A).

During an arc, while individual cells are being driven positive in voltage, it is expected that a cell's conductance jumps from α_i to α_e as the cell passes the plasma potential and back again on the negative swing. Unfortunately, such voltage-dependent conductance switches are beyond the scope of the present work. In this model, once floating equilibrium is established and all conductances determined prior to an arc, they are not permitted to change. It is possible, however, to partially explore the consequences of conductance switching and the resulting enhanced electron collection during an arc by using electron conductances somewhat greater than those expected physically.

Equivalent Circuits

Transient Response of a Chain of Cells

Figure 1 shows a transient circuit for a single chain of solar cells. Z_p is the impedance of the parallel combination of solar cell plasma capacitance C_p and resistance $1/\alpha$, and ρ and C have their previous definitions. An arc current injected at V_- flows toward V_+ and the load while leaking out to the plasma sheath along the way. The load transient is developed as the sum of the voltage transients across the cells due to the current transients through them.

Since current flowing in a chain toward V_+ is diminished by leakage to the sheath through the Z_p's, cell voltage transients also diminish in this direction. Thus, if all the Z_p's were placed in parallel at V_+, an overestimate of the load transient would result because all the cells would see the maximum current. Similarly, placing all the Z_p's at V_- would result in no load transient. These two cases bound the actual, uniform distribution case. An appropriate mixture of these cases approximates the actual one.

Using a mixture of the bounding cases results in a considerable simplification of the plasma interaction circuits. The Z_p's in each chain are split into two groups,

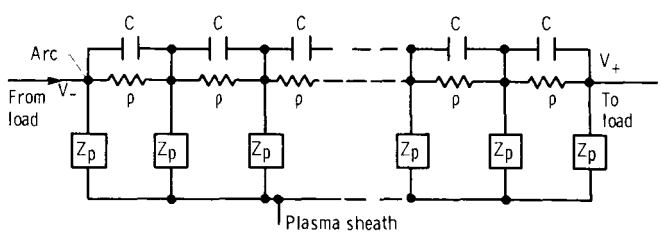

Figure 1.—Cell chain transient circuit.

one placed at V_- and the other at V_+, and the groups are combined in parallel at each terminal. A *plasma split* parameter δ adjusts the relative numbers of Z_p's at each terminal while keeping the whole constant (see appendix A). Ranging this parameter permits continuous variation from one bounding case to the other. Figure 2 shows the mixed-case circuit for a single chain of cells.

Solar Array Equivalent Circuit

Figure 3 shows the resultant solar array power system transient circuit used in the model. R_+, R_-, C_+, and C_- are plasma interaction components whose values are determined as described in appendix A. $C_o = MC/N$ and ρ_o and R_L have their previous definitions (see the **Solar Cell and Solar Array Characteristics** section).

As shown in appendix B, the terminal transient voltages, v_+ and v_-, satisfy a set of coupled, first-order differential equations with the arc pulse $i_s(t)$ as current driver. The equations can be solved for arbitrary $i_s(t)$ by the method of Laplace transforms. With

$$i_s(t) = I_o\left[\exp\left(\frac{-t}{T}\right) - \exp\left(\frac{-Kt}{T}\right)\right]$$

the time-domain solutions have the form

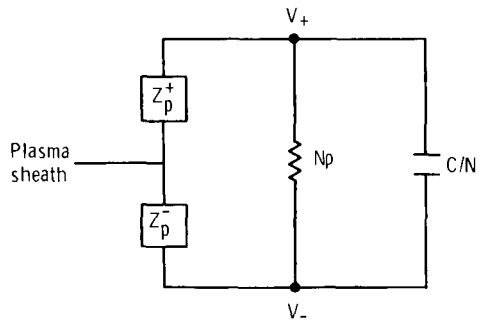

Figure 2.—Mixed-case single chain.

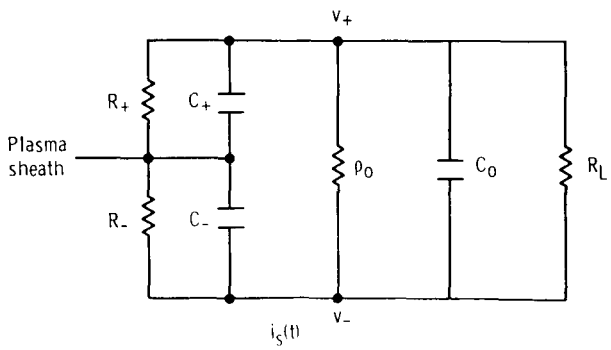

Figure 3.—Array transient circuit.

$$v(t) = B_1 \exp\left(\frac{-Kt}{T}\right) + B_2 \exp\left(\frac{-t}{T}\right) + B_3 \exp(\lambda_1 t)$$

$$+ B_4 \exp(\lambda_2 t) \qquad (4)$$

where B_1 ... B_4, λ_1, and λ_2 are functions of the circuit parameters and of I_o, K, and T. With $K > 1$, the driving current pulses have approximately the same time dependence as do the arcs seen in laboratory tests.

Although an alternate parameterization of the arcs using an *R-L-C* series circuit is possible, the I_o, T, and K parameterization is more directly comparable to experimental measurements.

Results and Discussion

Figures 4 to 8 show typical numerical results produced by the model. In the figures, v_- is the voltage transient amplitude at the negative end of the array and v_d is the load transient amplitude. The values $N = 1000$, $M = 1500$, $K = 5$, $\alpha_e = 2.4 \times 10^{-6}$ mho, and $\alpha_i = 2.10^{-8}$ mho apply throughout. Q is the total charge released, i.e., the integral of $i_s(t)$. The arc current amplitude I_o is limited to 200 A to insure the validity of the solar cell characteristic linearization (see the **Solar Cell and Solar Array Characteristics** section).

Figure 4 shows the first-quadrant solar cell characteristic curve used. Operating points for various fractions of maximum power are shown. The sharply increasing negative slope to the right of the maximum power operating point suggests that transient amplitudes per unit arc current should be larger in this region than they are at operating points to the left of the maximum power point where the slope and, hence, the dynamic

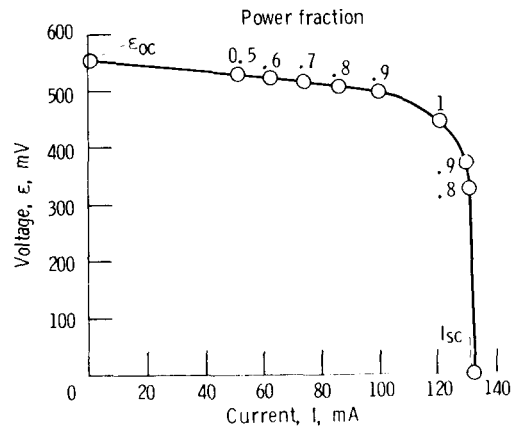

Figure 4.—Solar cell characteristic. Open-circuit voltage, ε_{oc}, 550 mV; short-circuit current, I_{sc}, 132 mA; voltage at maximum power, ε_{max}, 450 mV; current at maximum power, I_{max}, 122 mA; maximum power, P_{max}, 55 mW.

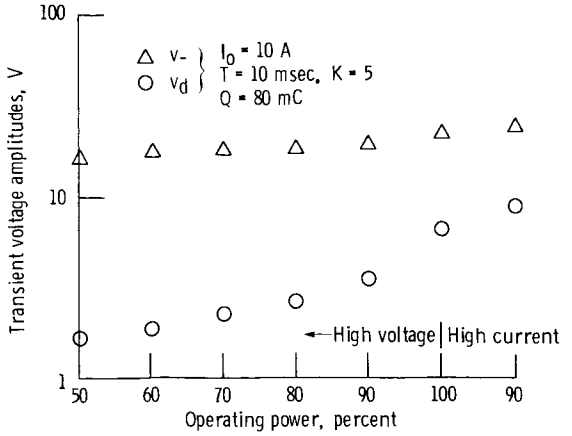

Figure 5.—Transient amplitudes as function of maximum power fraction.

resistance is smaller. Figure 5, which shows transient voltage amplitudes as a function of operating power for typical conditions, bears this out. There is a factor of almost three between values of v_d at the 90-percent points on either side of maximum power. This shows that transient amplitudes can be reduced significantly by operating on the high-voltage side of maximum power.

Amplitudes shown in figures 6 to 8 have been calculated assuming operation at 80-percent power in the high-voltage side. Figure 4 shows that solar cell linearization is a good approximation at this operating point if cell current transients are kept below about 30 mA; $I_o < 200$ A achieves this.

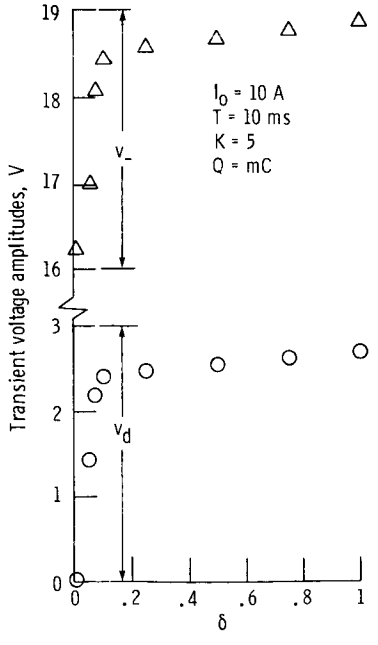

Figure 6.—Transient amplitudes as function of plasma split parameter δ. Arc current amplitude, I_o, 10 A; arc pulse fall time, T, 10 msec; K, 5; total charge released, Q, 80 mC.

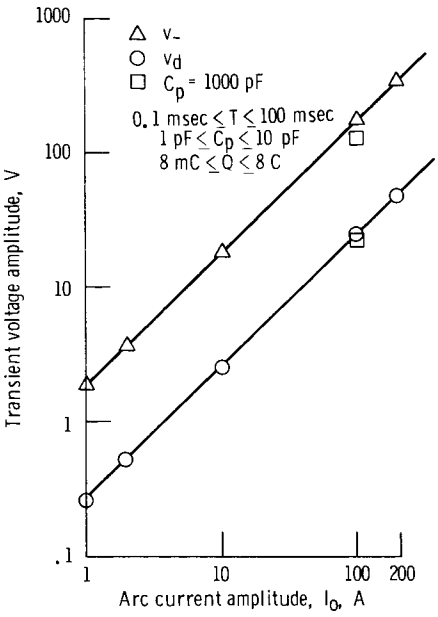

Figure 7.—Transient amplitudes for time T in milliseconds.

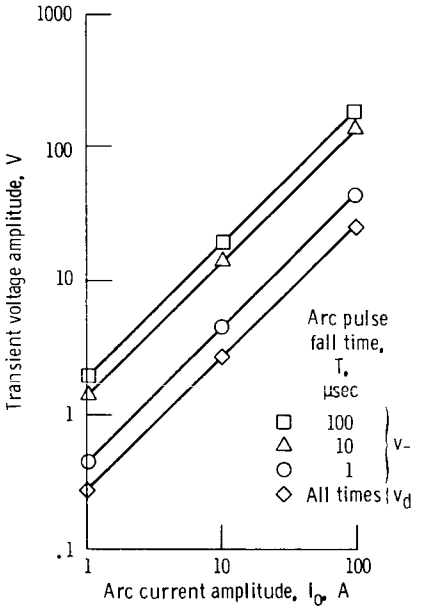

Figure 8.—Transient amplitudes for time T in microseconds. Equivalent capacitance per cell, C_p, 1 pF.

Figure 6 shows the effect of the plasma split parameter δ. $\delta = 1$ corresponds to $C_- = 1/R_- = 0$ and $\delta = 0$, for which v_d vanishes as it should, corresponds to $C_+ = 1/R_+ = 0$. (See appendix A.) Amplitudes decrease gradually with decreasing δ and then vary sharply when δ is small. This is because the equilibrium electron conductances are concentrated in a small region near V_+ where they are all assigned when δ is large. Large values of δ redistribute only the much weaker ion conductances and leave the conductance at V_+ constant. Only when δ

becomes less than about 0.08, which is the fraction of the array initially floating positive, do the large electron conductances at V_+ begin to shift to V_- and cause distributional effects to be seen in the transients.

Figures 7 and 8 show results for two regions of T, the arc pulse fall-time constant. The linear variation with I_o merely reflects that the solutions are explicitly proportional to I_o. In figure 7, v_- and v_d are seen to be nearly proportional to I_o, with little dependence on T and C_p. This is because T is much larger than circuit time constants (e.g., R_+C_+ or C_oR_L) so the circuit acts mainly like a series pair of resistors driven by $i_s(t)$. In figure 8, however, where T is of the order of R_+C_+, some dependence on T is seen in v_-.

The values of v_d in figures 7 and 8 show consistently the relation $v_d/I_o \approx 0.2$ ohm. This means that, for the present array parameters, load transients equal in amplitude to only 8 percent of the terminal voltage are produced by arcs of 200-A amplitude. Such arcs need only last 0.5 msec to transfer 80 mC of charge from an array to the plasma. This amount of charge is expected to be stored on a 1000 by 1500 cell array operating at 508 V and floating electrically in LEO.

Conclusions

The model presented here is intended to provide a simple means for estimating the transient response of high-voltage solar arrays in LEO to negative bias arcs. An analytical formulation has been made possible for both the plasma interactions and the solar cell characteristics by linear approximations. The model is a first step toward more complex analytical and numerical analyses of solar array transient behavior.

An especially needed addition to the model is an independently determined current/voltage characteristic for negative bias arcs. Introducing this to the circuit equations would permit determination of current and voltage transients free of arbitrary parameters. Without it, the model can calculate results only for given pulses. For the special conditions treated, pulses within the limits of the linear approximations of the model are not found to cause clearly unacceptable load transients. An estimation of the effects of stronger arcs awaits a nonlinear analysis.

Even if arc current amplitudes are small enough to cause only negligible single transients, many small arcs might combine to form an essentially continuous discharge. This could clamp the negative end of an array at or near the arc voltage threshold, which is a few hundred volts negative. The resulting enhanced electron collection due to snap-over at the positive end of a high voltage array could cause significant power losses (see **Plasma Current Collection**, p. 2). This effect needs further study.

National Aeronautics and Space Administration
Lewis Research Center
Cleveland, Ohio 44135, September 19, 1984

Appendix A— Calculation of Plasma Interaction Components

Calculation of Floating Equilibrium

For a chain with as many as 1000 cells, the voltage distribution V along the chain may be approximated by a continuous function of position. If $\epsilon(i)$ is the current/voltage characteristic of a cell and z locates a point in the chain, then

$$\frac{d^2V}{dz^2} = \left(\frac{d\epsilon}{di}\right)\left(\frac{di}{dz}\right) \qquad \text{for } 0<z<N \tag{A1}$$

Let the point z_o divide the chain into ion and electron collection regions. Thus, $V(z_o)$ is the plasma potential, here taken to be zero. For ion collection at $z<z_o$, $V<0$ and $di=-\alpha_i V\,dz$ in the ohmic approximation. For electron collection at $z>z_o$, $di=-\alpha_e V\,dz$ and $V>0$. As defined previously, $\alpha_i=z\times10^{-8}$ and $\alpha_e=2.4\times10^{-6}$ mho. If the slight variation of cell operating point along the chain is ignored, the cells have a common dynamic resistance, $d\epsilon/di=-\rho$. Substituting these expressions into equation (1) yields

$$\left.\begin{aligned} &\frac{d^2V}{dz^2}-\rho\alpha_i V=0 \qquad \text{for } z<z_o \\ &\frac{d^2V}{dz}-\rho\alpha_e V=0 \qquad \text{for } z>z_o \end{aligned}\right\} \tag{A2}$$

With the condition that V be continuous at z_o, the solution is

$$\left.\begin{aligned} &V=\frac{A\lambda_e \sinh\lambda_i}{\lambda_i}(z-z_o) \qquad \text{for } z<z_o \\ &V=A\sinh\lambda_e(z-z_o) \qquad \text{for } z>z_o \end{aligned}\right\} \tag{A3}$$

where $\lambda_e=(\rho\alpha_e)^{1/2}$, $\lambda_i=(\rho\alpha_i)^{1/2}$, and A is arbitrary. Current balance is achieved by requiring that ion and electron currents be equal. Thus,

$$-\int_0^{z_o}\alpha_i V\,dz=\int_{z_o}^{N}\alpha_e V\,dz \tag{A4}$$

which, using equation (A3), yields the condition

$$\cosh\lambda_i z_o=\cosh\lambda_e(N-z_o) \tag{A5}$$

Solving this gives

$$\frac{z_o}{N}=\frac{1}{\left(1+\frac{\lambda_i}{\lambda_e}\right)}=\frac{1}{1+\left(\frac{\alpha_i}{\alpha_e}\right)^{1/2}} \tag{A6}$$

With $\alpha_e=2.4\times10^{-6}$ mho and $\alpha_i=2\times10^{-8}$ mho, $z_o/N=0.92$. Thus, 8 percent of the chain floats above the plasma potential. For ram ions, with $\alpha_r=10^{-8}$ mho, $z_o/N=0.94$.

These results are unaffected by increasing the number of chains from 1 to M. With M chains, a factor of M would multiply both α_i and α_e in equation (A6), leaving it unchanged.

Plasma Interaction Distribution

Let δ be the fraction of an array whose plasma impedances Z_p are added together in parallel at the positive terminal V_+. Thus, δ is the plasma split parameter (see p. 4). Let $\gamma=z_o/N$. Then the following lumped circuit elements obtain at the terminals in the mixed-case approximation:

Capacitance:

$$C_+=\delta NMC_p$$

$$C_-=(1-\delta)NMC_p$$

Resistance:

For $\delta\le\gamma$,

$$\frac{1}{R_+}=\delta NM_e$$

$$\frac{1}{R_-}=NM\left|(\gamma-\delta)\alpha_e+(1-\gamma)\alpha_i\right|$$

For $\delta\ge\gamma$,

$$\frac{1}{R_-}=(1-\delta)NM\alpha_i$$

$$\frac{1}{R_+}=\left|\gamma\alpha_e+(\delta-\gamma)\alpha_i\right|NM$$

Appendix B—Circuit Analysis

The circuit of figure 3 obeys the following set of transient equations with initial conditions $v_+(0) = v_-(0) = 0$:

$$a_1\frac{dv_+}{dt} + a_2 v_+ - c\frac{dv_-}{dt} - f v_- = 0$$

$$b_1\frac{dv_-}{dt} + b_2 v_- - c\frac{dv_+}{dt} - f v_+ = i_s(t) \tag{B1}$$

where

$$a_1 = C_+ + C_o \qquad c = C_o$$

$$b_1 = C_- + C_o \qquad f = \frac{1}{R_o}$$

$$a_2 = \frac{1}{R_+} + \frac{1}{R_o} \qquad R_o = \frac{\rho_o R_L}{\rho_o + R_L}$$

$$b_2 = \frac{1}{R_-} + \frac{1}{R_o}$$

If the Laplace transform

$$q(s) = \mathcal{L}v(t) = \int_0^\infty e^{-st} v(t)\, dt$$

is used, equations (B1) form a pair of first-order algebraic equations in the variable s. The solutions for q_+ and q_- are

$$q_+(s) = p(s)\frac{cs+f}{D}; \quad q_-(s) = p(s)\frac{a_1 s + a_2}{D} \tag{B2}$$

where

$$p(s) = \mathcal{L}i_s(t)$$

$$D = (b_1 s + b_2)(a_1 s + a_2) - (cs + f)^2$$

The denominator D may be put in the form

$$D = A(s - \lambda_1)(s - \lambda_2)$$

where $A = b_1 a_1 - c^2$ and the λ's are solutions of the equation $D = 0$. The transforms for q_+ and q_- may be inverted using well known theorems with the following results (ref. 9):

$$v_+ = [1/A(\lambda_1 - \lambda_2)]\int_0^t [(c\lambda_1 + f)\exp(\lambda_1\tau) - (c\lambda_2 + f) \times \exp(\lambda_2\tau)]\, i_s(t-\tau)\, d\tau \tag{B3}$$

and v_- is the same but with c and f replaced by a_1 and a_2, respectively. These are the solutions for arbitrary $i_s(t)$ provided $i_s(0) = 0$. Let us take the special case

$$i_s(t) = I_o(e^{-t/T} - e^{-Kt/T}) \qquad \text{for } K > 1 \tag{B4}$$

Then, doing the integral in equation (B3) gives

$$v_+(t) = \left(\frac{I_o}{A}\right)\left(B_1 e^{-tK/T} + B_2 e^{-t/T} + B_3 e^{\lambda_1 t} + B_4 e^{\lambda_2 t}\right)$$

where

$$B_1 = \frac{\frac{cK}{T} - f}{\left(\lambda_1 + \frac{K}{T}\right)\left(\lambda_2 + \frac{K}{T}\right)}$$

$$B_2 = \frac{-\left(\frac{c}{T} - f\right)}{\left(\lambda_1 + \frac{1}{T}\right)\left(\lambda_2 + \frac{1}{T}\right)}$$

$$B_3 = (K-1)\frac{c\lambda_1 + f}{\left(\lambda_1 - \lambda_2\right) T\left(\lambda_1 + \frac{1}{T}\right)\left(\lambda_1 + \frac{K}{T}\right)}$$

$$B_4 = -(K-1)\frac{c\lambda_2 + f}{\left(\lambda_1 - \lambda_2\right) T\left(\lambda_2 + \frac{1}{T}\right)\left(\lambda_2 + \frac{K}{T}\right)} \tag{B5}$$

The expression for v_- is identical but with c and f replaced by a_1 and a_2. From v_+ and v_- one can easily construct the load transient $v_+ - v_-$.

Let us consider a simple but useful limit to the previous solutions. Suppose that the solar array internal capacitance C_o is so small that it can be neglected and that all the plasma impedance is at the positive terminal, i.e., $\delta = 1$. Then, with $C_- = 1/R_- = 0$ and the limit $C_o \to 0$ taken last, one finds

$$v_+(t) = I_o R_+ T\left[\frac{e^{-Kt/T}}{(K\tau_+ - T)} - \frac{e^{-t/T}}{(\tau_+ - T)} + \frac{(K-1)\tau_+ e^{-t/\tau_+}}{(\tau_+ - T)(K\tau_+ - T)}\right] \tag{B6}$$

and

$$v_+(t) - v_-(t) = -I_o R_o(e^{-t/T} - e^{-Kt/T}) = -R_o i_s(t)$$

where $\tau_+ = R_+ C_+$. This expression for the load transient ($v_+ - v_-$) is to be expected since, with $C_o = 0$, the arc current flows through a pure resistance R_o. In actual practice, C_o is quite small and equation (B6) gives a rough estimate of transient amplitudes.

References

1. Stevens, N. John: Review of Biased Solar Array–Plasma Interaction Studies. NASA TM-82693, 1981.
2. Grier, Norman T.: Dilute Plasma Coupling Currents to a High Voltage Solar Array in Weak Magnetic Fields. NASA TM-83687, 1984.
3. Snyder, David B.: Discharges on a Negatively Biased Solar Array in a Charged Particle Environment. NASA TM-83644, 1983.
4. Leung, P.: Discharge Characteristics of a Simulated Solar Cell Array. IEEE Trans. Nuc. Sci., vol. 30, no. 6, Dec. 1983, pp. 4311–4315.
5. Purvis, Carolyn K.; Stevens, N. John; and Berkopec, Frank D.: Interaction of Large, High Power Systems With Operational Orbit Charged Particle Environments. NASA TM-73867, 1977.
6. Rauschenbach, Hans S.: Solar Cell Array Design Handbook. Van Nostrand Reinhold, 1980, pp. 52 to 56.
7. Smith, Robert E.; and West, George S.: Space and Planetary Environment Criteria Guidelines for Use in Space Vehicle Development, 1982 Revision, Vol. 1. NASA TM-82478, 1983.
8. Chen, Francis F.: Electric Probes. Plasma Diagnostic Techniques, Richard N. Huddlestone and Stanley L. Leonard, eds., Academic Press, 1965, pp. 113 to 200.
9. Selby, Samuel M., ed.: CRC Standard Mathematical Tables. 21st ed. CRC Press, 1973, pp. 506 to 515.

1. Report No.	2. Government Accession No.	3. Recipient's Catalog No.
NASA TP-2407		

4. Title and Subtitle	5. Report Date
Circuit Transients Due to Negative Bias Arcs on a High-Voltage Solar Array in Low Earth Orbit	January 1985
	6. Performing Organization Code 506-55-72

7. Author(s)	8. Performing Organization Report No.
Roger N. Metz	E-2239
	10. Work Unit No.

9. Performing Organization Name and Address	11. Contract or Grant No.
National Aeronautics and Space Administration Lewis Research Center Cleveland, Ohio 44135	
	13. Type of Report and Period Covered Technical Paper

12. Sponsoring Agency Name and Address	14. Sponsoring Agency Code
National Aeronautics and Space Administration Washington, D.C. 20546	

15. Supplementary Notes

Roger N. Metz, Colby College, Waterville, Maine, and Resident Research Associate at Lewis Research Center (work partially funded by Colby College).

16. Abstract

Arcing to negatively biased, exposed solar cell interconnects on solar arrays placed in plasma environments has been well established in laboratory tests and inferred from space data. Such arcing may cause damaging interference with the operation of electrical power systems in spacecraft planned to be driven with high-voltage solar arrays. A simple analytical model has been developed to estimate the effects of negative bias arcs on solar array power system performance. Solar cell characteristics, plasma interactions, and power system features are modeled approximately by a linear, lumped element transient circuit, and the time domain equations are solved. Exact numerical results for solar array common-mode and load voltage transients are calculated for typical conditions. Acceptable load transients are found for a range of arc current amplitudes and time constants.

17. Key Words (Suggested by Author(s))	18. Distribution Statement
High-voltage solar array Circuit transients Negative bias arcs	Unclassified - unlimited STAR category 18

19. Security Classif. (of this report)	20. Security Classif. (of this page)	21. No. of pages	22. Price*
Unclassified	Unclassified	11	A02

*For sale by the National Technical Information Service, Springfield, Virginia 22161

NASA-Langley, 1985